Published in final edited form as:
Biochim Biophys Acta. 2015 January ; 1854(1): 31–38. doi:10.1016/j.bbapap.2014.09.019.

Kinetic analysis of PCNA clamp binding and release in the clamp loading reaction catalyzed by *Saccharomyces cerevisiae* replication factor C

Melissa R. Marzahn[1], **Jaclyn N. Hayner**, **Jennifer A. Meyer**, and **Linda B. Bloom**[2]
1600 SW Archer Road, P.O. Box 100245, Department of Biochemistry & Molecular Biology, University of Florida, Gainesville, FL 32610-0245, USA

Abstract

DNA polymerases require a sliding clamp to achieve processive DNA synthesis. The toroidal clamps are loaded onto DNA by clamp loaders, members of the AAA+ family of ATPases. These enzymes utilize the energy of ATP binding and hydrolysis to perform a variety of cellular functions. In this study, a clamp loader-clamp binding assay was developed to measure the rates of ATP-dependent clamp binding and ATP-hydrolysis-dependent clamp release for the *S. cerevisiae* clamp loader (RFC) and clamp (PCNA). Pre-steady-state kinetics of PCNA binding showed that although ATP binding to RFC increases affinity for PCNA, ATP binding rates and ATP-dependent conformational changes in RFC are fast relative to PCNA binding rates. Interestingly, RFC binds PCNA faster than the *Escherichia coli* γ complex clamp loader binds the β-clamp. In the process of loading clamps on DNA, RFC maintains contact with PCNA while PCNA closes, as the observed rate of PCNA closing is faster than the rate of PCNA release, precluding the possibility of an open clamp dissociating from DNA. Rates of clamp closing and release are not dependent on the rate of the DNA binding step and are also slower than reported rates of ATP hydrolysis, showing that these rates reflect unique intramolecular reaction steps in the clamp loading pathway.

Keywords

DNA replication; clamp loader; sliding clamp; replication factor C (RFC); proliferating cell nuclear antigen (PCNA); AAA+ ATPase

1. INTRODUCTION

Sliding clamps are toroidal proteins that encircle duplex DNA and tether the DNA polymerase to the template DNA, thereby reducing the number of binding events and

[2]To whom correspondence should be addressed: Phone: 352-392-8708, Fax: 352-392-6511, lbloom@ufl.edu.
[1]Current address: Department of Structural Biology, St. Jude Children's Research Hospital, Memphis, TN 38105

limiting dissociation. Thus, the speed of DNA synthesis is limited by rates of nucleotide incorporation (reviewed in [1]). In eukaryotes, the replicative sliding clamp, proliferating cell nuclear antigen (PCNA), is a homotrimer of subunits arranged in a head-to-tail fashion [2–4]. PCNA is required not only for DNA replication but also for a variety of other cellular functions including DNA repair pathways, chromatin remodeling, and sister chromatid cohesion (reviewed in [5]). In each case, a clamp loader is required to load PCNA onto DNA. The primary clamp loader required for DNA replication, replication factor C (RFC), is a heteropentameric complex belonging to the AAA+ family of ATPases [6–10]. These molecular motors use the energy from ATP binding and hydrolysis to load clamps onto DNA (reviewed in [11]). The clamp loading reaction is complex, involving many steps and conformational changes in the clamp loader and clamp. Simplistically, RFC, in the presence of ATP, binds to the clamp and DNA, forming an intermediate ternary complex [12–18]. Formation of this complex causes conformational changes that induce ATP hydrolysis, causing RFC to release PCNA onto DNA [17,19–23]. However, many individual kinetic steps are required to complete a single clamp loading reaction cycle. In this study, we have developed a fluorescence-based assay to measure RFC-PCNA binding interactions specifically. This method was used to characterize ATP-dependent binding of RFC to PCNA and to compare the relative rates of PCNA closing around DNA to PCNA dissociation from RFC during a productive clamp loading reaction.

2. MATERIALS AND METHODS

2. 1. Buffers and reagents

RFC assay buffer consists of 30 mM HEPES pH 7.5, 150 mM sodium chloride (NaCl), 2 mM dithiothreitol (DTT), 10 mM magnesium chloride ($MgCl_2$), and 10% glycerol. γ complex assay buffer consists of 20 mM Tris-HCl pH 7.5, 50 mM NaCl, 8 mM $MgCl_2$, and 10% glycerol. PCNA storage buffer contains 30 mM HEPES pH 7.5, 0.5 mM EDTA, 2 mM DTT, 150 mM NaCl, and 10% glycerol. RFC storage buffer is the same as for PCNA except the NaCl concentration was increased to 300 mM. Storage buffers for γ complex and β-pyrene (β-PY) are as reported previously [24].

Concentrations of ATP (GE Healthcare) diluted with 30 mM HEPES pH 7.5 were determined from the absorbance at 259 nm and using an extinction coefficient of 15,400 M^{-1} cm^{-1}.

2. 2. Proteins

RFC and PCNA expression vectors were provided by M. O'Donnell and colleagues (Rockefeller University) [25,26]. RFC containing a truncated Rfc1 protein, lacking the first 283 amino acids, was expressed as previously described [27–29]. Site-directed mutagenesis of the PCNA coding sequence converted naturally occurring Cys residues 22, 62, and 81 to Ser, Ser-43 to Cys for labeling the binding mutant, and Ile-111 and Ile-181 to Cys for labeling the opening mutant as previously reported [30]. PCNA was expressed, purified, and labeled as previously described [2,30,31] with minor modifications. RFC was expressed and purified as previously described [25,26,32] with minor modifications. The γ complex clamp loader subunits γ [33], δ [34], δ′ [34], and χψ [35], were purified, and the γ complex ($\gamma_3\delta\delta$

′χψ) was reconstituted [36], as previously described. The β clamp was purified [37] and labeled with pyrene [24] as previously described.

2. 3. Steady-state fluorescence assays

All steady-state measurements were made and analyzed as described previously [38]. Final concentrations were 0.5 mM ATP, 5, 10, or 20 nM PCNA-MDCC, and 0–400 nM RFC. Average values and standard deviations for three independent experiments are reported and the average relative intensities and standard deviations were plotted and fit using Kaleidagraph [38]. Dissociation constants (K_d) were calculated using equation 1 where R_o and P_o are the total concentrations of RFC and PCNA-MDCC, respectively, and I_{max} and I_{min} are the maximum and minimum MDCC intensities, respectively.

$$I_{obs}=\frac{K_d+R_o+P_o-\sqrt{(K_d+R_o+P_o)^2-4R_oP_o}}{2P_o}*(I_{max}-I_{min})+I_{min} \quad (1)$$

Competition-binding of RFC to PCNA-MDCC versus unlabeled wild-type PCNA (wt PCNA) was done by adding reagents sequentially to a cuvette starting with assay buffer with ATP followed by PCNA-MDCC and unlabeled wt PCNA, and finally, RFC. Final concentrations were: 0.5 mM ATP, 20 nM PCNA-MDCC, 0 – 400 nM wt PCNA, and 20 nM RFC. Emission spectra were corrected for background by subtracting the buffer signal. Relative MDCC intensities were calculated from the ratio of emission at 467 nm for PCNA-MDCC with RFC to PCNA-MDCC without RFC, and plotted as a function of wt PCNA concentration and fit to equation (2) using Kaleidagraph [38]. In equation 2, $PCNA_{MDCC}$ is the concentration of PCNA-MDCC (20 nM), $PCNA_{wt}$ is the concentration of wt unlabeled PCNA, I_{max} is MDCC intensity in the absence of wt PCNA (set to a value of 1) and I_{min} is the signal at saturating concentrations of wt PCNA (fit as an adjustable parameter, calculated value of 0.74 ± 0.11) [30].

$$I_{obs}=\left(\frac{PCNA_{MDCC}}{PCNA_{MDCC}+PCNA_{wt}}\right)*(I_{\max}-I_{\min})+I_{\min} \quad (2)$$

2. 4. Pre-steady-state kinetic measurements

Assays were performed using an Applied PhotoPhysics SX20MV stopped-flow apparatus at 20°C. MDCC emission fluorescence was monitored using a 455 nm cut-on filter while exciting at 420 nm. Pyrene emission fluorescence was monitored using a 365 nm cut-on filter while exciting at 345 nm. Alexa Fluor 488 emission was monitored using a 515 nm cut-on filter while exciting at 495 nm. For clamp binding assays, experiments were performed in single mix mode, mixing equal volumes (60μL) of two solutions containing reactants in assay buffer. For clamp closing and release assays, experiments were performed in sequential mix mode, in which a solution of RFC was mixed with a solution of PCNA and ATP prior to adding a solution of DNA and ATP. Eight or more individual kinetic traces were averaged. The time courses were corrected for background by subtracting the signal for buffer. For PCNA release and closing assays, a solution of RFC, labeled PCNA, and ATP

was added to a solution of wt PCNA, DNA (when present), and ATP at concentrations indicated in Figure legends. Time courses were normalized to the intensity at the start of the reaction. The rate of change in fluorescence, k_{obs}, was fit to a single exponential decay [38]. For clamp binding reactions, a solution of clamp loader (RFC or γ complex) and ATP was added to a solution of labeled clamp (PCNA-MDCC or β-PY) and ATP at concentrations indicated in Figure legends. Data were collected for a total of 4 seconds at 0.4 ms intervals. Time courses were divided by fluorescence of the free clamp to give relative fluorescence increases, and fit to double exponential rises (γ complex/β) or single exponential rises (RFC/PCNA) using Kaleidagraph [38] to calculate observed rate constants, k_{obs}.

3. RESULTS

3. 1. Equilibrium RFC•PCNA binding

A fluorescence intensity-based assay was developed to measure clamp binding by RFC during the clamp loading cycle. A surface residue on PCNA, Ser-43, was mutated to Cys to covalently label this site with MDCC (Figure 1A). Three of the four naturally occurring Cys residues, 22, 62, and 81, in PCNA were converted to Ser to allow for selective labeling of Cys-43 [30]. The fourth naturally occurring Cys residue should not be solvent accessible for labeling under these conditions [3]. The predicted RFC “footprint” on PCNA upon binding is such that RFC may interact with two or more of the fluorophores [4,39–41] (Figure 1A). When RFC binds PCNA-MDCC, MDCC fluorescence increases by about three-fold (Figures 1B & C).

Using this assay, RFC binding to PCNA was measured under equilibrium conditions in assays with ATP. Three separate titrations were done at three different PCNA concentrations (Figure 1C). Dissociation constants, K_d values, for RFC-PCNA-MDCC were calculated from these data using equation 1. Average K_d values from the three independent experiments were 5.5 ± 1.9 nM, 7.9 ± 0.5 nM, and 9.6 ± 2.3 nM for 5 (blue), 10 (black), and 20 (orange) nM PCNA-MDCC, respectively. These values are in agreement with one another with an average of 7.7 ± 2.3 nM for the nine measurements. This K_d is within the same order of magnitude as the value of 1.3 nM measured in a single surface plasmon resonance experiment [14] and the values of 2.6 to 4.5 nM measured in clamp closing assays [30].

To determine whether the mutations introduced into PCNA for labeling affected interactions with RFC, a competition-binding assay was performed in which unlabeled wild-type (wt) PCNA competed for RFC binding with PCNA-MDCC. In this assay, 20 nM RFC was added to solutions of 20 nM PCNA-MDCC and increasing concentrations of wt PCNA (Figure 1D). The decrease in MDCC fluorescence with increasing unlabeled PCNA can be adequately fit to equation 2, which simply takes into account the fraction of total PCNA that is labeled with MDCC, demonstrating that RFC binds with equal affinity to both PCNA-MDCC and unlabeled wt PCNA. Together, these data show that RFC binds PCNA-MDCC with same affinity as wt PCNA.

3. 2. Pre-steady-state PCNA binding by RFC with and without ATP preincubation

The PCNA-MDCC binding assay was used to determine the rate constant for RFC binding PCNA. In these experiments, a pre-incubated solution of RFC and 0.5 mM ATP was was rapidly mixed with a solution of PCNA-MDCC and 0.5 mM ATP (Figure 2A). The rate of the increase in MDCC fluorescence increased with increasing concentration of RFC as expected for a biomolecular binding reaction. The first second of reaction time courses were fit to single exponential rises to calculate observed rates, k_{obs}, for binding (solid black lines through reaction traces), and these k_{obs} values were plotted as a function of RFC concentration in Figure 2C. A linear fit of these k_{obs} plots yields apparent on-rate constants, $k_{on(app)}$, from the slopes [24]. The average of three independent stopped-flow experiments gave a value of $k_{on(app)} = 1.4 \pm 0.5 \times 10^8$ $M^{-1}s^{-1}$ for RFC binding PCNA-MDCC. Thus, RFC binds PCNA rapidly at a rate limited by diffusion.

Given that ATP binding to the clamp loader promotes conformational changes in the clamp loader that increase its affinity for the clamp and DNA to drive the clamp loading reaction, an experiment was done to determine whether ATP-induced conformational changes would be reflected in the rate of clamp binding. In this experiment, a solution of RFC was rapidly mixed with a solution of PCNA-MDCC and 1 mM ATP (to yield a final concentration of 0.5 mM ATP) in reactions in which RFC was not pre-incubated with ATP (Figure 2B). Observed rates, k_{obs}, for binding (solid black lines through reaction traces) were calculated from single exponential fits and these k_{obs} values are plotted along with those for the ATP-preincubated reactions in Figure 2C for comparison. An apparent $k_{on(app)}$ value of 1.1×10^8 $M^{-1}s^{-1}$ was calculated from the average of linear fits of two independent experiments. The binding rates are the same within experimental error whether or not RFC is pre-incubated with ATP, showing that ATP-dependent conformational changes do not limit the rate of RFC-PCNA binding.

3. 3. Comparison of clamp binding kinetics by the *S. cerevisiae* and *E. coli* clamp loaders

The rate at which RFC binds PCNA measured in Figure 2 is about six times faster than the rate reported for the *E. coli* clamp loader, γ complex, binding to the β-clamp [24]. To determine whether this difference in rates is real, or instead reflects differences in reaction conditions such as glycerol concentrations that affect viscosity, side-by-side clamp binding reactions were performed with RFC and the γ complex. A solution of clamp loader (RFC or γ complex) and 0.5 mM ATP was rapidly mixed with a solution of labeled clamp (PCNA-MDCC or β-PY) and 0.5 mM ATP (Figure 3). Both reactions contained 10% glycerol. Time courses for reactions containing 20 nM clamp and 200 nM clamp loader are plotted on the same graph to highlight the difference in rates. The data from the first second of the time course for γ complex binding β was fit to a double exponential rise [24,42] and for RFC and PCNA to single exponential rise to calculate apparent rates, k_{obs}. Unlike the case for MDCC fluorescence, PY fluorescence is sensitive to both the clamp binding and clamp opening steps [42], and therefore, the β-PY binding time course requires a double exponential fit. RFC binding to PCNA occurred at a rate of 36 s^{-1} while the rate of γ complex binding to β-PY was 5.5 s^{-1}. Thus, RFC binds PCNA about 6.5 times faster than γ complex binds β [24], which is in good agreement with the difference in $k_{on(app)}$ rates measured in the two different studies.

3. 4. PCNA is closed prior to release onto DNA by RFC

The decrease in MDCC fluorescence that occurs when PCNA-MDCC dissociates from RFC can be used to follow clamp loading onto DNA. In these reactions, RFC was preincubated with PCNA-MDCC and ATP in assay buffer to form an open clamp loader-clamp complex, and this solution was rapidly mixed with a solution of DNA, unlabeled PCNA, and ATP in assay buffer (Figure 4A, red trace). Unlabeled PCNA was kept in excess to limit the reaction to a single observable turnover. To determine whether this assay can distinguish between *passive* dissociation of the clamp loader from the clamp or *active* clamp release onto DNA due to clamp loading, an identical reaction was performed except that DNA was omitted so that only passive dissociation is possible (Figure 4A, blue trace). The time courses for both reactions were fit to single exponential decays (Figure 4A, solid black lines) to estimate rates of clamp release of 0.048 s^{-1} and 0.31 s^{-1} for passive dissociation (blue trace) and active clamp loading (red trace), respectively. The rate of passive dissociation agrees with the rate of 0.035 s^{-1} reported by Gomes, *et al*. as measured by SPR [14]. The time course for the clamp loading reaction is not a simple exponential decay (or sum of exponentials), but instead has a more sigmoidal shape with a short lag prior to the decrease in fluorescence, whereas the time course for passive clamp dissociation corresponds to a simple exponential decay (consistent with a simple dissociation event). The more complex shape of the clamp loading time course reflects additional reaction steps, e.g. RFC-PCNA binding DNA and RFC hydrolyzing ATP, that are “invisible” in terms of MDCC fluorescence. Overall, clamp loading is about 6-fold faster than passive clamp release and can be distinguished kinetically from passive dissociation.

DNA binding triggers the release of PCNA from RFC during the clamp loading reaction. To determine whether the kinetics of PCNA release depend on this second-order DNA binding step, clamp release rates were measured as a function of DNA concentration, 20 (red), 40 (blue), and 100 (gray) nM DNA. The observed rates of clamp release were the same at each DNA concentration (k_{obs} = 0.41 ± 0.04 s^{-1}) (Figure 4B) showing that the rate of clamp release is limited by the rate of an intramolecular reaction in the RFC-PCNA-DNA complex.

In previous work, we developed a PCNA opening/closing assay in which PCNA is labeled on both sides of each monomer interface with Alexa Fluor 488 (PCNA-$AF488_2$) [30]. When PCNA is closed, the AF488 molecules interact and self-quench, and when RFC opens PCNA, two AF488 molecules are separated and increase in fluorescence. This closing assay was done “side-by-side” with the clamp release assay to determine whether PCNA “snaps” shut when released by RFC onto DNA or whether PCNA closes prior to dissociation from RFC (Figure 4C). For both reactions, a pre-incubated solution of RFC, fluorescently labeled PCNA (either PCNA-MDCC or PCNA-$AF488_2$), and ATP was mixed with a solution of DNA and excess unlabeled PCNA at final concentrations listed in the figure legend. Thus, an open clamp loader-clamp complex was added to DNA. The decrease in AF488 fluorescence that occurs on clamp closing (black trace, k_{close} = 2.2 s^{-1}) is nearly 10-fold faster than the decrease in MDCC fluorescence that occurs on clamp release (blue trace, $k_{release}$ = 0.26 s^{-1}) (Figure 4C), showing that PCNA closes before it is released on DNA by RFC. As with release rates, PCNA closing rates are also independent of DNA concentration (k_{obs} = 6.4 ± 1.5 s^{-1}) and time courses are more sigmoidal in shape than exponential (Figure

4D). Hence, both the rates of clamp closing and release are limited by a reaction that occurs after DNA binding and the formation of a RFC-PCNA-DNA complex. These data show that PCNA closes before dissociating from RFC.

4. DISCUSSION

The clamp loading reaction is quite complex in that at least a dozen steps are required to describe a simple linear reaction pathway [13,15,21,23,43–45]. These steps include binding 4 or 5 molecules of ATP, clamp binding, clamp opening, DNA binding, ATP hydrolysis, clamp closing, clamp release, DNA release, ADP/P_i dissociation, and at least two conformational changes in RFC induced by ATP binding and hydrolysis. “Branches” in the pathway are also likely, adding further complexity. Given this number of variables, assays are needed to measure as many individual interactions and reactions as possible to reliably define a kinetic mechanism for the clamp loading reaction pathway. In this paper, we have developed a fluorescence-based assay to measure RFC-PCNA binding and dissociation reactions.

ATP binding to clamp loaders drives the clamp loading reaction by increasing the affinity of the clamp loader for the clamp and DNA, and by stabilizing an open conformation of the clamp [12,14–16,42,46,47]. These ATP-induced conformational changes in the clamp loader likely increase contacts between RFC and PCNA to increase affinity and stabilize an open conformation as demonstrated by the differences in a *closed* RFC-PCNA complex in comparison and an *open* bacteriophage T4 clamp loader•clamp complex [4,39,41]. To determine whether ATP-induced conformational changes in RFC would be reflected in rates of PCNA binding, rates for PCNA-MDCC binding were measured in reactions in which ATP was added to RFC at the same time as PCNA (Figure 2). If ATP-induced conformational changes were a pre-requisite for PCNA binding, then the rate of RFC-PCNA-MDCC binding would increase with RFC concentration until a concentration at which the rate of the conformational changes was slower and became rate-limiting. However, in these reactions, RFC-PCNA binding rates increased linearly with RFC concentration and did not approach a saturating value limited by the rate of an intramolecular reaction. The apparent binding rate was the same whether or not RFC was fully equilibrated with ATP or was added to PCNA and ATP simultaneously, and both occurred at diffusion controlled limits. Thus, the rate of ATP-induced conformational changes in RFC does not limit the rate of RFC-PCNA binding. This could be because ATP-induced conformational changes are extremely rapid and occur much faster than RFC-PCNA binding at the highest RFC concentrations measured. Or given that PCNA binding is a two-step reaction in which RFC binds PCNA, and PCNA opens in the second step [30,47], another interesting possibility is that ATP-induced conformational changes may not be required for initial RFC-PCNA binding, but instead may occur after a RFC-PCNA complex forms to support the clamp opening reaction.

In vitro, RFC equilibrated with ATP can bind either PCNA or DNA first [15], however, given the topology of the macromolecules in the cell, it is unlikely that a ternary RFC-PCNA-DNA could form if RFC bound DNA before PCNA. One way to favor PCNA binding prior to DNA binding would be a kinetic preference for binding PCNA faster than

DNA. This is observed in the *E. coli* system where a relatively slow ATP-induced conformational change in the clamp loader limits the rate of DNA binding but not β-clamp binding so that clamp binding is faster [24]. As for the β-clamp, the rate of PCNA binding to RFC is not limited by the rate of ATP-induced conformational changes in RFC suggesting that RFC may also have a kinetic preference for binding PCNA before DNA. In support of this model, kinetic analyses show a slow ATP-dependent activation of RFC occurs before DNA binding [44]. Thus, ATP-induced conformational changes in RFC may not be required for an initial PCNA binding step such that this step is rapid, but instead may be facillitating the PCNA opening step along with DNA binding.

To uncover similarities and differences in mechanisms of clamp loading across domains of life, we directly compared the *E. coli* and *S. cerevisiae* clamp loaders, γ complex and RFC, respectively. The affinity of each of the clamp loaders for the clamps is similar: a K_d value of 7.7 ± nM was measured here using the PCNA-MDCC binding assay and a K_d value of 3.2 ± 0.9 nM was measured for *E. coli* γ complex binding β by SPR [48]. Although both RFC and γ complex bind clamps with similar affinities, the rate at which RFC binds PCNA is about 6 to 7 times faster than the rate at which γ complex binds β (Figure 3). Pre-steady-state analysis of PCNA binding by RFC measured here yielded a bi-molecular binding rate constant of $1.4 \pm 0.3 \times 10^8$ M^{-1} s^{-1} compared to the rate of 2.3×10^7 $M^{-1}s^{-1}$ for γ complex binding the β-clamp [24]. The differences in the binding rates may reflect the differences in the symmetry of the clamps. β is a homodimer whereas PCNA is a homotrimer, such that RFC can productively bind PCNA in three possible orientations, whereas the γ complex can only bind β in two productive orientations. Although RFC binds PCNA faster than γ complex binds β, previous studies have shown that PCNA opening (2 s^{-1}) is about 4 to 5 times slower than β opening (9 s^{-1}) [30,42,47]. Both clamp loaders form open clamp loader-clamp complexes in a two-step reaction in which clamp binding occurs prior to clamp opening [30,42,47], thus the faster binding rate of RFC is counterbalanced by a slower opening rate such that the overall rates of binding/opening reactions are similar.

Given the stability of PCNA as a closed ring [49,50], it is quite possible that RFC simply releases PCNA and PCNA rapidly “snaps” shut around DNA. In this type of mechanism, interactions between positively charged amino acid residues that line the center of the clamp and negatively charged phosphates of DNA could stabilize PCNA on DNA to prevent PCNA dissociation prior to closure [3,51,52]. However, this mechanism leaves open the possibility that PCNA could dissociate from DNA before closing. To determine whether PCNA rapidly shuts after dissociation from RFC, or PCNA closes around DNA prior to dissociating from RFC, rates of PCNA closing and release were measured under identical conditions. These experiments directly showed that PCNA closes around DNA faster than PCNA dissociates from RFC (Figure 4C). Thus, the clamp loader does not leave open the possibility that an open clamp could dissociate from DNA before the clamp closes. Both the rates of PCNA closing and PCNA release are independent of DNA concentration (Figure 4B and D) showing that they are not dependent on the rate of the second order DNA binding, but dependent on the rate of an intramolecular reaction in the clamp loader•clamp•DNA complex. Given that PCNA is closing is faster than PCNA release, the steps that govern the rates of these two reactions differ. This kinetic order of events is conserved in bacteria

where the *E. coli* clamp closes around DNA faster than it is released by the clamp loader [53]. Interestingly, the rate of PCNA-MDCC release onto DNA as the result of clamp loading is about five times slower than previously reported for PCNA loading/release [23]. The most likely explanation for this difference is that different measurements were made in the two studies. In this study, PCNA dissociation was monitored directly via the decrease in MDCC fluorescence, whereas Chen *et al*. monitored DNA release instead, and assumed that PCNA was released at the same time. If both studies are interpreted together, then this would mean that RFC releases DNA before PCNA. The same order of events has been proposed for the *E. coli* clamp loading reaction [54]. By combining results from this study and from Chen *et al.* [44], a likely series of events that occurs after formation of a ternary RFC•PCNA•DNA complex is: ATP is hydrolyzed, PCNA closes, DNA is released, and finally the clamp is released. This highlights the importance of developing specific assays to measure as many of the individual interactions and reactions in the clamp-loading pathway as possible to arrive at a kinetic mechanism that is consistent with all of the measurements.

5. CONCLUSIONS

Clamp loading, particularly on the lagging strand, must be efficient to keep pace with the advancing replication fork. Although the replication fork moves about ten times faster in bacteria than eukaryotes, Okazaki fragments are about ten times longer in bacteria so the rapid frequency with which clamps must be loaded on the lagging strand is similar in both. Our kinetic analysis of RFC-PCNA interactions highlights two mechanisms that contribute to efficient clamp loading. First, RFC binds PCNA at diffusion-controlled rates whether or not RFC has been pre-incubated with ATP. Not only does this ensure a rapid binding reaction, but this also increases the probability that RFC binds PCNA prior to DNA because DNA binding is limited by a slower ATP-dependent RFC activation step [44]. Furthermore, if RFC were to bind DNA first, the topology of the proteins and DNA would likely prevent the RFC•DNA complex from binding a closed clamp. In this case, RFC-DNA binding would trigger ATP hydrolysis by RFC resulting in a futile cycle reducing the overall efficiency of the clamp loading reaction. Second, the efficiency of the clamp loading reaction is further enhanced by PCNA closure prior to dissociation of RFC from PCNA. By maintaining an interaction with the clamp and DNA until PCNA closes, RFC reduces the possibility that an open clamp dissociates from DNA prior to closing limiting unproductive clamp loading events as a result.

Acknowledgments

We thank Mike O'Donnell and his colleagues for recombinant RFC and PCNA expression plasmids.

FUNDING

This research is supported by NIH Grant R01 GM082849 (LBB) and the Training Grant in Cancer Biology T32CA009126-32 (JNH).

Abbreviations used

RFC	replication factor C

PCNA	proliferating cell nuclear antigen
DTT	dithiothreitol
$MgCl_2$	magnesium chloride
EDTA	ethylenediaminetetraacetic acid
MDCC	N-(2-(1-maleimidyl)ethyl)-7-(diethylamino)coumarin-3-carboxamide
PCNA-MDCC	PCNA labeled with MDCC
PY	pyrene
β-PY	β labeled with pyrene
K_d	dissociation constant
SPR	surface plasmon resonance

References

1. McHenry CS. DNA replicases from a bacterial perspective. Annu Rev Biochem. 2011; 80:403–436. [PubMed: 21675919]
2. Bauer GA, Burgers PM. The yeast analog of mammalian cyclin/proliferating-cell nuclear antigen interacts with mammalian DNA polymerase delta. Proc Natl Acad Sci USA. 1988; 85:7506–7510. [PubMed: 2902631]
3. Krishna TS, Kong XP, Gary S, Burgers PM, Kuriyan J. Crystal structure of the eukaryotic DNA polymerase processivity factor PCNA. Cell. 1994; 79:1233–1243. [PubMed: 8001157]
4. Bowman GD, O'Donnell M, Kuriyan J. Structural analysis of a eukaryotic sliding DNA clamp-clamp loader complex. Nature. 2004; 429:724–730. [PubMed: 15201901]
5. Maga G, Hübscher U. Proliferating cell nuclear antigen (PCNA): a dancer with many partners. J Cell Sci. 2003; 116:3051–3060. [PubMed: 12829735]
6. Tsurimoto T, Stillman B. Purification of a cellular replication factor, RF-C, that is required for coordinated synthesis of leading and lagging strands during simian virus 40 DNA replication *in vitro*. Mol Cell Biol. 1989; 9:609–619. [PubMed: 2565531]
7. Tsurimoto T, Stillman B. Functions of replication factor C and proliferating-cell nuclear antigen: functional similarity of DNA polymerase accessory proteins from human cells and bacteriophage T4. Proc Natl Acad Sci USA. 1990; 87:1023–1027. [PubMed: 1967833]
8. Lee SH, Kwong AD, Pan ZQ, Hurwitz J. Studies on the activator 1 protein complex, an accessory factor for proliferating cell nuclear antigen-dependent. DNA polymerase delta. 1991; 266:594–602.
9. Cullmann G, Fien K, Kobayashi R, Stillman B. Characterization of the five replication factor C genes of *Saccharomyces cerevisiae*. Mol Cell Biol. 1995; 15:4661–4671. [PubMed: 7651383]
10. Neuwald AF, Aravind L, Spouge JL, Koonin EV. AAA+: A class of chaperone-like ATPases associated with the assembly, operation, and disassembly of protein complexes. Genome Res. 1999; 9:27–43. [PubMed: 9927482]
11. Duderstadt KE, Berger JM. AAA+ ATPases in the initiation of DNA replication. Crit Rev Biochem Mol Biol. 2008; 43:163–187. [PubMed: 18568846]
12. Turner J, Hingorani MM, Kelman Z, O'Donnell M. The internal workings of a DNA polymerase clamp-loading machine. EMBO J. 1999; 18:771–783. [PubMed: 9927437]
13. Alley SC, Abel-Santos E, Benkovic SJ. Tracking sliding clamp opening and closing during bacteriophage T4 DNA polymerase holoenzyme assembly. Biochemistry. 2000; 39:3076–3090. [PubMed: 10715129]
14. Gomes XV, Burgers PM. ATP utilization by yeast replication factor C. I. ATP-mediated interaction with DNA and with proliferating cell nuclear antigen. 2001; 276:34768–34775.

15. Gomes XV, Schmidt SL, Burgers PM. ATP utilization by yeast replication factor C. II. Multiple stepwise ATP binding events are required to load proliferating cell nuclear antigen onto primed. DNA. 2001; 276:34776–34783.
16. Hingorani MM, O'Donnell M. ATP binding to the *Escherichia coli* clamp loader powers opening of the ring-shaped clamp of DNA polymerase III holoenzyme. 1998; 273:24550–24563.
17. Sexton DJ, Kaboord BF, Berdis AJ, Carver TE, Benkovic SJ. Dissecting the order of bacteriophage T4 DNA polymerase holoenzyme assembly. Biochemistry. 1998; 37:7749–7756. [PubMed: 9601035]
18. Zhuang Z, Berdis AJ, Benkovic SJ. An alternative clamp loading pathway via the T4 clamp loader gp44/62-DNA complex. Biochemistry. 2006; 45:7976–7989. [PubMed: 16800623]
19. Berdis AJ, Benkovic SJ. Role of adenosine 5′-triphosphate hydrolysis in the assembly of the bacteriophage T4 DNA replication holoenzyme complex. Biochemistry. 1996; 35:9253–9265. [PubMed: 8703931]
20. Young MC, Weitzel SE, von Hippel PH. The kinetic mechanism of formation of the bacteriophage T4 DNA polymerase sliding clamp. J Mol Biol. 1996; 264:440–452. [PubMed: 8969296]
21. Hingorani MM, Bloom LB, Goodman MF, O'Donnell M. Division of labor--sequential ATP hydrolysis drives assembly of a DNA polymerase sliding clamp around DNA. Embo J. 1999; 18:5131–5144. [PubMed: 10487764]
22. Bertram JG, Bloom LB, Hingorani MM, Beechem JM, O'Donnell M, Goodman MF. Molecular mechanism and energetics of clamp assembly in *Escherichia coli*. The role of ATP hydrolysis when gamma complex loads beta on DNA. 2000; 275:28413–28420.
23. Chen S, Levin MK, Sakato M, Zhou Y, Hingorani MM. Mechanism of ATP-driven PCNA clamp loading by *S. cerevisiae* RFC. J Mol Biol. 2009; 388:431–442. [PubMed: 19285992]
24. Thompson JA, Paschall CO, O'Donnell M, Bloom LB. A slow ATP-induced conformational change limits the rate of DNA binding but not the rate of beta clamp binding by the *Escherichia coli* gamma complex clamp loader. 2009; 284:32147–32157.
25. Johnson A, Yao NY, Bowman GD, Kuriyan J, O'Donnell M. The replication factor C clamp loader requires arginine finger sensors to drive DNA binding and proliferating cell nuclear antigen loading. 2006; 281:35531–35543.
26. Finkelstein J, Antony E, Hingorani MM, O'Donnell M. Overproduction and analysis of eukaryotic multiprotein complexes in *Escherichia coli* using a dual-vector strategy. Anal Biochem. 2003; 319:78–87. [PubMed: 12842110]
27. Uhlmann F, Cai J, Gibbs E, O'Donnell M, Hurwitz J. Deletion analysis of the large subunit p140 in human replication factor C reveals regions required for complex formation and replication activities. 1997; 272:10058–10064.
28. Podust VN, Tiwari N, Stephan S, Fanning E. Replication factor C disengages from proliferating cell nuclear antigen (PCNA) upon sliding clamp formation, and PCNA itself tethers DNA polymerase delta to DNA. 1998; 273:31992–31999.
29. Gomes XV, Gary SL, Burgers PM. Overproduction in *Escherichia coli* and characterization of yeast replication factor C lacking the ligase homology domain. 2000; 275:14541–14549.
30. Thompson JA, Marzahn MR, O'Donnell M, Bloom LB. Replication factor C is a more effective proliferating cell nuclear antigen (PCNA) opener than the checkpoint clamp loader, Rad24-RFC. J Biol Chem. 2012; 287:2203–2209. [PubMed: 22115746]
31. Ayyagari R, Impellizzeri KJ, Yoder BL, Gary SL, Burgers PM. A mutational analysis of the yeast proliferating cell nuclear antigen indicates distinct roles in DNA replication and DNA repair. Mol Cell Biol. 1995; 15:4420–4429. [PubMed: 7623835]
32. Yao N, Coryell L, Zhang D, Georgescu RE, Finkelstein J, Coman MM, et al. Replication factor C clamp loader subunit arrangement within the circular pentamer and its attachment points to proliferating cell nuclear antigen. 2003; 278:50744–50753.
33. Maki S, Kornberg A. DNA polymerase III holoenzyme of *Escherichia coli*. I. Purification and distinctive functions of subunits tau and gamma, the dnaZX gene products. 1988; 263:6547–6554.
34. Dong Z, Onrust R, Skangalis M, O'Donnell M. DNA polymerase III accessory proteins I holA and holB encoding delta and delta′. 1993; 268:11758–11765.

35. Olson MW, Dallmann HG, McHenry CS. DnaX complex of *Escherichia coli* DNA polymerase III holoenzyme. The chi psi complex functions by increasing the affinity of tau and gamma for delta.delta′ to a physiologically relevant range. 1995; 270:29570–29577.
36. Onrust R, Finkelstein J, Naktinis V, Turner J, Fang L, O'Donnell M. Assembly of a chromosomal replication machine: two DNA polymerases, a clamp loader, and sliding clamps in one holoenzyme particle. I Organization of the clamp loader. 1995; 270:13348–13357.
37. Johanson KO, Haynes TE, McHenry CS. Chemical characterization and purification of the beta subunit of the DNA polymerase III holoenzyme from an overproducing strain. 1986; 261:11460–11465.
38. Marzahn MR, Hayner JN, Finkelstein J, O'Donnell M, Bloom LB. The ATP sites of AAA+ clamp loaders work together as a switch to assemble clamps on DNA. 2014; 289:5537–5548.
39. Tainer JA, McCammon JA, Ivanov I. Recognition of the ring-opened state of proliferating cell nuclear antigen by replication factor C promotes eukaryotic clamp-loading. J Am Chem Soc. 2010; 132:7372–7378. [PubMed: 20455582]
40. Bowman GD, Goedken ER, Kazmirski SL, O'Donnell M, Kuriyan J. DNA polymerase clamp loaders and DNA recognition. FEBS Lett. 2005; 579:863–867. [PubMed: 15680964]
41. Kelch BA, Makino DL, O'Donnell M, Kuriyan J. How a DNA polymerase clamp loader opens a sliding clamp. Science. 2011; 334:1675–1680. [PubMed: 22194570]
42. Paschall CO, Thompson JA, Marzahn MR, Chiraniya A, Hayner JN, O'Donnell M, et al. The *Escherichia coli* Clamp Loader Can Actively Pry Open the β-Sliding Clamp. J Biol Chem. 2011; 286:42704–42714. [PubMed: 21971175]
43. Trakselis MA, Alley SC, Abel-Santos E, Benkovic SJ. Creating a dynamic picture of the sliding clamp during T4 DNA polymerase holoenzyme assembly by using fluorescence resonance energy transfer. Proc Natl Acad Sci USA. 2001; 98:8368–8375. [PubMed: 11459977]
44. Sakato M, Zhou Y, Hingorani MM. ATP binding and hydrolysis-driven rate-determining events in the RFC-catalyzed PCNA clamp loading reaction. J Mol Biol. 2012; 416:176–191. [PubMed: 22197378]
45. Kumar R, Nashine VC, Mishra PP, Benkovic SJ, Lee TH. Stepwise loading of yeast clamp revealed by ensemble and single-molecule studies. Proc Natl Acad Sci USA. 2010; 107:19736–19741. [PubMed: 21041673]
46. Ason B, Bertram JG, Hingorani MM, Beechem JM, O'Donnell M, Goodman MF, et al. A model for *Escherichia coli* DNA polymerase III holoenzyme assembly at primer/template ends. DNA triggers a change in binding specificity of the gamma complex clamp loader. 2000; 275:3006–3015.
47. Zhuang Z, Yoder BL, Burgers PMJ, Benkovic SJ. The structure of a ring-opened proliferating cell nuclear antigen-replication factor C complex revealed by fluorescence energy transfer. Proc Natl Acad Sci USA. 2006; 103:2546–2551. [PubMed: 16476998]
48. Naktinis V, Onrust R, Fang L, O'Donnell M. Assembly of a chromosomal replication machine: two DNA polymerases, a clamp loader, and sliding clamps in one holoenzyme particle. II. Intermediate complex between the clamp loader and its clamp. 1995; 270:13358–13365.
49. Yao N, Turner J, Kelman Z, Stukenberg PT, Dean F, Shechter D, et al. Clamp loading, unloading and intrinsic stability of the PCNA, beta and gp45 sliding clamps of human, *E. coli* and T4 replicases. Genes Cells. 1996; 1:101–113. [PubMed: 9078370]
50. Binder JK, Douma LG, Ranjit S, Kanno DM, Chakraborty M, Bloom LB, et al. Intrinsic stability and oligomerization dynamics of DNA processivity clamps. Nucleic Acids Res. 2014; 42:6476–6486. [PubMed: 24728995]
51. McNally R, Bowman GD, Goedken ER, O'Donnell M, Kuriyan J. Analysis of the role of PCNA-DNA contacts during clamp loading. BMC Struct Biol. 2010; 10:3. [PubMed: 20113510]
52. Zhou Y, Hingorani MM. Impact of individual proliferating cell nuclear antigen-DNA contacts on clamp loading and function on DNA. 2012; 287:35370–35381.
53. Hayner JN, Bloom LB. The β Sliding Clamp Closes around DNA prior to Release by the *Escherichia coli* Clamp Loader γ Complex. J Biol Chem. 2013; 288:1162–1170. [PubMed: 23161545]

54. Anderson SG, Thompson JA, Paschall CO, O'Donnell M, Bloom LB. Temporal correlation of DNA binding, ATP hydrolysis, and clamp release in the clamp loading reaction catalyzed by the *Escherichia coli* gamma complex. Biochemistry. 2009; 48:8516–8527. [PubMed: 19663416]

HIGHLIGHTS

- ATP binding-dependent conformational changes in RFC are fast relative to PCNA binding.
- Rates of sliding clamp binding are faster for the *S. cerevisiae* than the *E. coli* clamp loader.
- PCNA closes faster than dissociation from RFC preventing dissociation of an open clamp from DNA.
- Rates of clamp closing and release reflect unique kinetic steps in the clamp loading pathway.

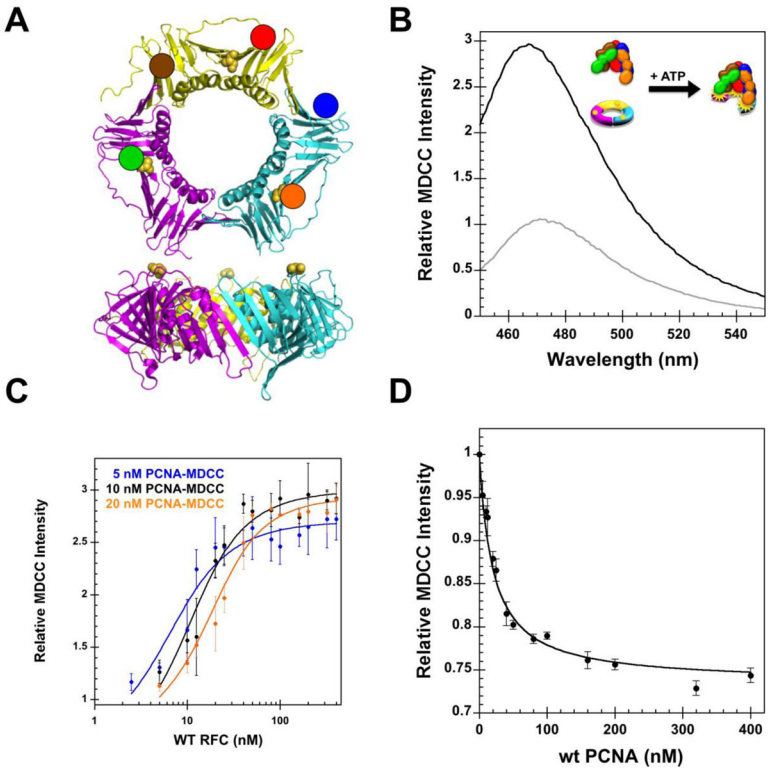

Figure 1. PCNA-MDCC binding assay to measure equilibrium RFC•PCNA binding

(A) Ribbon diagrams of PCNA (monomers colored magenta, yellow, and cyan) viewed from the face that binds RFC with the predicted "footprint" of RFC indicated by colored circles (upper image) and from the edge (lower image) (PDB ID: 1SXJ [4]). Ser-43, which was mutated to Cys and labeled with MDCC, is shown as yellow spheres. (B) Emission spectra of 10 nM PCNA-MDCC with (black trace) and without (gray trace) 400 nM RFC is shown. (C) The increase in MDCC fluorescence when RFC binds PCNA-MDCC is plotted for the average of three independent experiments with standard deviations (error bars). Solid lines through data points represent a fit to equation 1 to calculate dissociation constants, K_d values. (D) Competition-binding of RFC to labeled PCNA–MDCC vs. unlabeled PCNA for reactions containing 20 nM PCNA-MDCC and 20 nM RFC is shown. The average relative MDCC intensity from three independent experiments is plotted with standard deviations (error bars). These data were fit to the fraction of labeled PCNA (equation 2).

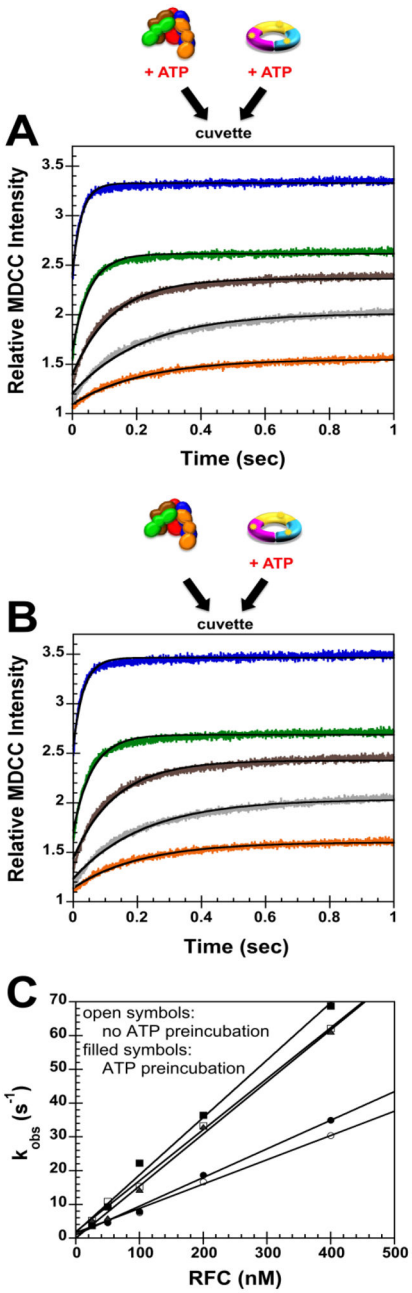

Figure 2. Pre-steady-state kinetics of RFC binding PCNA

(A) RFC was preincubated with ATP before rapidly mixing with a solution of PCNA-MDCC and ATP. (B) RFC alone was rapidly mixed with a solution of PCNA-MDCC and ATP. Final concentrations in panels A and B were the same: 20 nM PCNA-MDCC, 0.5 mM ATP, and 25 nM (orange), 50 nM (gray), 100 nM (brown), 200 nM (green), or 400 nM (blue) RFC in assay buffer. Increases in MDCC intensity as a function of time are empirically fit to single exponential rises (black lines through traces) to calculate observed rates. (C) Observed rates, k_{obs}, for data with ATP pre-incubation from panel A (filled symbols, three independent experiments) and without ATP pre-incubation panel B (open

symbols, two independent experiments) are plotted against the concentration of RFC. A linear fit of the data gives the apparent rate constant, $k_{on,app}$ (slope).

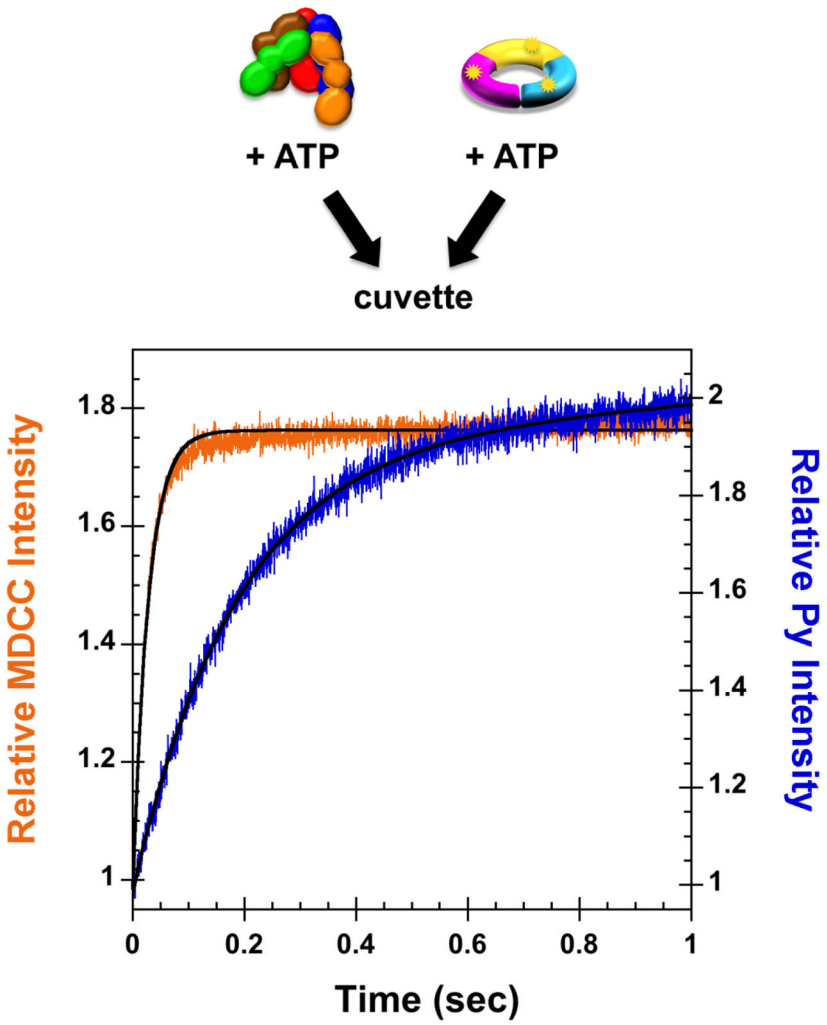

Figure 3. Comparison of clamp binding rates for *S. cerevisiae* RFC and *E. coli* γ complex

A diagram of the stopped-flow mixing scheme is shown above the graph. The increase in MDCC intensity when RFC binds PCNA-MDCC (orange trace) and the increase in PY intensity when γ complex binds β-PY (blue) are plotted on the same time scale. Solid black lines through the time courses are the result of an empirical fit of the data to a single exponential rise for RFC•PCNA and to a double exponential rise for γ complex•β to calculate observed rates.

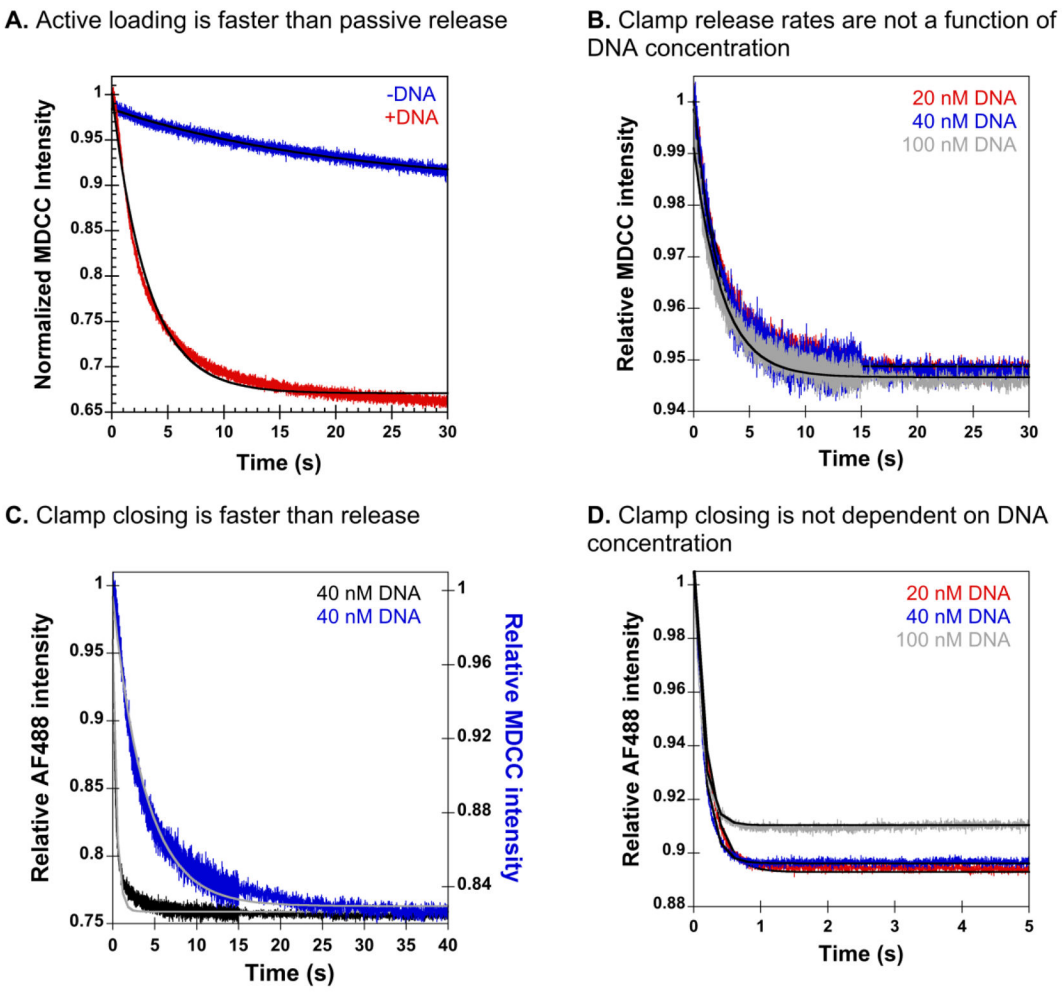

Figure 4. PCNA clamp closing is faster than PCNA release by RFC

PCNA closing and PCNA release were measured in real time when a solution of RFC, labeled PCNA and ATP was added to a solution of DNA and unlabeled PCNA trap. All reactions contained 20 nM RFC, 20 nM PCNA, 0.5 mM ATP, 200 nM unlabeled PCNA and DNA concentrations indicated. Data were empirically fit to single exponential decays to calculate rates. (A) The blue trace shows a reaction in which DNA was omitted (*passive release*) and red trace shows a reaction that contains DNA (*active clamp loading*). (B) PCNA-MDCC release onto DNA was measured as a function of DNA concentration. (C) PCNA-AF488$_2$ closing and PCNA-MDCC release on DNA were measured under identical conditions. (D) PCNA-AF488$_2$ closing was measured as a function of DNA concentration.